

Evidence for Basolateral P2Y₆ Receptors along the Rat Proximal Tubule: Functional and Molecular Characterization

MATTHEW A. BAILEY,* MARTINE IMBERT-TEBOUL,§ CLARE TURNER,*
S. KAILA SRAI,† GEOFFREY BURNSTOCK,‡ and ROBERT J. UNWIN*‡

*Centre for Nephrology, †Department of Biochemistry and Molecular Biology, and ‡Autonomic Neuroscience Institute, Royal Free and University College Medical School, University College London, London, United Kingdom; and §Centre National de la Recherche Scientifique URA 1859, CEA Saclay, Gif sur Yvette, France.

Abstract. In this study, the distribution of P2Y₆ receptor mRNA in rat nephron segments was investigated and a functional approach was used to analyze basolateral protein expression. Reverse transcription-PCR studies revealed more intense expression of P2Y₆ receptor mRNA in the proximal tubule and the thick ascending limb of Henle's loop, less intense expression in the thin descending limb and the cortical and outer medullary collecting ducts, and no detectable expression in either the thin ascending limb or the inner medullary collecting duct. Dose-dependent calcium responses to basolateral administration of UDP (a selective agonist for the P2Y₆ receptor) were observed in the proximal tubule but not in any of the other segments studied. In the proximal tubule, intracellular calcium concentration changes induced by UDP were associated with increased production of inositol phosphates, as were those

induced by ATP and norepinephrine. However, UDP-induced intracellular calcium concentration changes were different, exhibiting no plateau after the initial peak; moreover, a single stimulation with a high concentration of UDP induced full desensitization of the UDP-sensitive calcium pathway but did not alter the responsiveness of the proximal tubule to ADP (a specific P2Y₁ receptor agonist), ATP, or norepinephrine. In summary, this report demonstrates that P2Y₆ receptor mRNA is expressed in most segments of the rat nephron but that basolateral expression of the protein is restricted to the proximal tubule, where the receptor is coexpressed with the P2Y₁ receptor. The differences in the distributions of P2Y₆ receptor mRNA and UDP responses may indicate the presence of luminal receptors in other nephron segments.

A recent report demonstrated that several cell types, including epithelial cells, release significant amounts of UTP (1). This suggests that uridine compounds, such as UTP and UDP, are potentially important extracellular signaling molecules. The uridine-activated receptors, *i.e.*, P2Y₂, P2Y₄, and P2Y₆ receptors, are subtypes within the larger P2Y receptor family, and these receptors are widely distributed in many tissues. UTP and ATP are equipotent at P2Y₂ and P2Y₄ receptors (2–4), whereas P2Y₆ receptors are preferentially activated by UDP, with ATP and ADP being only weakly active (5–7). Functionally, all of these receptors are coupled to phospholipase C (PLC), and activation leads to transient increases in the intracellular calcium concentration ($[Ca^{2+}]_i$) (8,9). As demonstrated by molecular and functional studies of cultured (10–17) and native (18–22) epithelial cells, several different P2Y subtypes are located in the luminal membrane, the basolateral membrane, or both membranes; these subtypes can be coex-

pressed in the same cells, all participating in the regulation of fluid and/or electrolyte transport.

In the kidney, reverse transcription-PCR (RT-PCR) studies have demonstrated the presence of P2Y₂ and P2Y₄ receptor mRNA in most segments of the nephron (23). Functional studies have also demonstrated that UTP and ATP generate calcium signals along the whole renal tubule (23–26); however, these agonists are equipotent at the rat P2Y₂ and P2Y₄ receptors, and whether the signals involve one or the other (or both) of these receptor subtypes cannot be determined. It is also not possible to know whether responses are mediated via apical or basolateral membrane receptors, because P2Y₂ receptor-specific immunoreactive sites were recently observed in both membranes of inner medullary collecting duct (IMCD) cells (27). In addition, ATP- and UTP-sensitive receptors were detected in both the luminal and basolateral membranes of the mouse cortical collecting duct (CCD) (28).

Relatively little is known regarding the function of P2Y₆ receptors, although recent reports suggested that UDP-sensitive receptors can activate ion channels in a variety of polarized epithelia, such as sweat gland (12,15,29), gallbladder (20), pancreatic duct (22), and nasal (13) cells. Northern hybridization studies detected P2Y₆ receptor mRNA expression in several different tissues (*e.g.*, spleen, placenta, thymus, intestine, and blood leukocytes), but expression was observed at a very low level in the kidney (5,6). However, it is possible that this receptor has only limited distribution within the nephron and

Received June 14, 2000. Accepted January 3, 2001.

Correspondence to Dr. Robert J. Unwin, Centre for Nephrology, Institute of Urology and Nephrology, The Middlesex Hospital, Mortimer Street, London, W1N 8AA, UK. Phone: 0207-504-9302; Fax: 0207-637-7006; E-mail: robert.unwin@ucl.ac.uk

1046-6673/1208-1640

Journal of the American Society of Nephrology

Copyright © 2001 by the American Society of Nephrology

that Northern analysis of whole-kidney extracts could not detect this. Therefore, the aim of this study was to screen for P2Y₆ receptors in segments of the rat nephron. The RT-PCR technique was used to study the distribution of mRNA; because specific antibodies directed against the rat P2Y₆ receptor are not yet available, we analyzed the functional expression of the protein by measuring inositol phosphate (IP) production and associated changes in $[Ca^{2+}]_i$ in response to UDP. Our results demonstrate that P2Y₆ receptor mRNA is expressed in most segments of the rat nephron but basolateral expression of the protein, as assessed functionally, is restricted to the proximal tubule, where the receptor is coexpressed with the P2Y₁ receptor.

Materials and Methods

Isolation of Rat Nephron Segments

The left kidneys of male Sprague-Dawley rats anesthetized with sodium pentobarbital (Nembutal; 50 mg/kg body wt, administered intraperitoneally) were perfused, via the renal artery, with 5 ml of Hepes-buffered saline solution (HBSS; 140 mM NaCl, 5 mM KCl, 0.8 mM MgSO₄, 0.33 mM Na₂HPO₄, 0.44 mM NaH₂PO₄, 1.0 mM MgCl₂, 1 mM CaCl₂, 10 mM Hepes, 5 mM NaOH, 5 mM glucose [pH 7.4]), followed by the same volume of a 0.16% collagenase solution (Serva; Boehringer Mannheim, Mannheim, Germany). Thin cortico-medullary slices were then incubated in 0.12% collagenase solution for 20 min at 30°C before segments were isolated in microdissection medium (HBSS to which 0.1% bovine serum albumin had been added) at 4°C. For proximal tubules, only non-collagenase-treated kidneys were used (isolated from rats of 90 to 100 g body wt), because collagenase treatment adversely affects responses to calcium-mobilizing agents. Pyruvate (1 mM), glycine (4 mM), and glutamate (2 mM) were included in the proximal tubule microdissection medium. All tubule samples were then stored in a droplet of microdissection medium (2 μl) at 0 to 4°C until use.

The following segments were studied: nonlocalized proximal convoluted tubules (PCT) taken from the kidney cortex or, when specified, S1 segments identified on the basis of functional criteria (see the Results section), proximal straight tubules taken from medullary rays along the S3 portion of the proximal tubules, type II thin descending limbs (DTL) of juxtamedullary nephrons, thin ascending limbs (ATL), cortical thick ascending limbs, medullary thick ascending limbs (MTAL), CCD, outer medullary collecting ducts (OMCD), and IMCD. DTL, MTAL, and OMCD were all isolated from the inner stripe of the outer medulla.

Extraction of mRNA

RNA was extracted from microdissected segments by using a micromethod (30) adapted from the guanidinium thiocyanate-phenol/chloroform method (31). Briefly, pools of individual segments were photographed for length determinations before being transferred, with 5 to 10 μl of microdissection medium, into 400 μl of denaturing solution (4 M guanidinium thiocyanate, 25 mM sodium citrate [pH 7.0], 0.5% sarcosyl, 0.1 mM β-mercaptoethanol, 20 μg of yeast tRNA). After phenol/chloroform extraction and isopropyl alcohol precipitation, the final pellet was vacuum-dried and resuspended in RNA dilution buffer [10 mM Tris-HCl [pH 7.6], 1 mM ethylenediaminetetraacetate, 2 mM dithiothreitol, 40 U/ml ribonuclease inhibitor (RNasin; Promega, Madison, WI)]. It was previously determined that the yield of this extraction procedure was >90% (30).

RT-PCR

Specific primers were selected from the sequence of the rat P2Y₆ receptor cDNA and from the sequence of the human glyceraldehyde-3-phosphate dehydrogenase (GAPDH) cDNA by using Oligo Primer analysis software (Medprobe, Oslo, Norway). The sequences of the P2Y₆ receptor primers were 5'-TGCTGGGTGGTATGTG-GAGTC-3' (positions 868 to 889) for the forward primer and 5'-TGGAAAGGCAGGAAGCTGATAAC-3' (positions 1206 to 1184) for the reverse primer. The sequences of the GAPDH primers were 5'-GCCATCAATGACCCCTTCAT-3' (positions 154 to 173) for the forward primer and 5'-GAGGGGGCAGAGATGATGAC-3' (positions 434 to 415) for the reverse primer.

For each segment, mRNA extracted from 1-mm tubule length (approximately 60 pg of mRNA) was reverse-transcribed for 50 min at 42°C with 0.5 μg of oligo(dT)_{12–18} primer, using a first-strand cDNA synthesis kit for RT-PCR (Superscript II RNase H⁻ reverse transcriptase; Invitrogen Ltd., Paisley, UK). After denaturation at 95°C for 3 min, the resulting product was used as a template with the PCR Core System I (Promega). For the P2Y₆ receptor, 40 PCR cycles were performed under the following conditions: 95°C for 30 s, 62°C for 1 min (annealing), and 72°C for 1 min (extension) for five cycles; 95°C for 30 s, 56°C for 1 min, and 72°C for 1 min for 34 cycles, with a last cycle with a 10-min extension stage. For GAPDH, only 30 cycles were performed, as follows: 95°C for 30 s, 55°C for 1 min, and 72°C for 1 min for 29 cycles, plus a last cycle with a 10-min extension stage.

The resulting PCR products were resolved on a 2% (wt/vol) agarose gel containing 10 μg/ml ethidium bromide and were observed under ultraviolet illumination. For the P2Y₆ receptor, the nature of the PCR product (expected size, 339 bp) was confirmed by sequencing (Oswel DNA Sequencing Laboratories, Southampton, UK). In all experiments, the presence of possible contaminants was investigated using control RT-PCR assays of samples in which either mRNA had been excluded (blank) or reverse transcriptase had been omitted from the RT mixture.

Measurement of $[Ca^{2+}]_i$

$[Ca^{2+}]_i$ was measured using previously described methods (32). Each tubular segment was loaded with fura2/acetoxymethyl ester (10 μM in microdissection medium; Molecular Probes, Eugene, OR) for 1 h at room temperature and was subsequently transferred to a superfusion chamber, where the ends of the segment were aspirated into two glass holding pipettes (to prevent possible perfusion of the luminal membrane). The segment was then superfused with HBSS, at a rate of 10 ml/min, for a 5-min equilibration period. Fura2 fluorescence was measured in a tubular portion of 20 to 30 cells, using a standard photometric configuration (model MSP 21; Zeiss, Jena, Germany), during superfusion with either HBSS alone or HBSS to which agonists had been added. All solutions were stored in individual reservoirs at room temperature until use; the temperature of each solution was increased to 37°C just before introduction into the perfusion chamber.

After subtraction of tubular autofluorescence from the fura2 fluorescence intensities at 340 and 380 nm, $[Ca^{2+}]_i$ was calculated using the equation presented by Grynkiewicz *et al.* (33), with a calcium dissociation constant for fura2 of 224 nM. The calibration parameters were determined from internal calibration assays using solutions containing 10 μM ionomycin and both 0 mM Ca²⁺ and 1 mM ethylene glycol bis(β-aminoethyl ether)-N,N,N',N'-tetraacetic acid (for the minimal ratio) or 3 mM Ca²⁺ (for the maximal ratio).

Measurement of Phosphoinositide Metabolism

The method used was previously described in detail (34,35). Briefly, well preserved pieces of proximal tubules (*i.e.*, a mixture of S1, S2, and S3 cortical fragments) were sorted from tubule suspensions prepared, by sieving, from non-collagenase-treated rat kidney cortex (35). OMCD were microdissected from collagenase-treated rat kidneys, as described above. All tubules were labeled for 2 h in HBSS (2 mM Ca^{2+}) containing 1 mCi/ml *myo*-[^3H]inositol (Amersham, Buckinghamshire, UK), in a humid atmosphere at 37°C.

After labeling, segments were extensively rinsed at room temperature under stereomicroscopic observation, for removal of extracellular *myo*-[^3H]inositol, and then batches of 10 segments (approximately 5-mm tubule length) were transferred, in 2 μl of HBSS, to glass test tubes containing 48 μl of HBSS (1 mM Ca^{2+}). Incubations with agonists were initiated by the addition of 50 μl of HBSS (1 mM Ca^{2+}) containing the agent (at double concentration) and LiCl (final concentration, 10 mM).

Reactions were terminated after 15 min by the addition of 940 μl of chloroform/methanol (1:2, vol/vol) and 200 μl of 5 mM Tris-ethylenediaminetetraacetate (pH 7.0). Water and chloroform (300 μl of each) were added to the reaction tube, which was then centrifuged for 5 min at $3000 \times g$ at 4°C for separation of the phases. For each sample, the upper hydrophilic phase was removed for chromatography, whereas 500 μl of water and 500 μl of methanol were added to the remaining hydrophobic phase. After vortex-mixing and repeat centrifugation, the lower phase, containing phosphoinositides (PI), was recovered and evaporated to dryness in counting vials before measurement of radioactivity.

Radioactivities associated with free inositol, glycerophosphoinositol (GPI), and IP were separated by chromatography, as described previously (35). Samples were applied to columns containing 0.25 g of Dowex AG1-X8 resin, and free inositol, GPI, and IP were successively and respectively eluted with the following: (1) 3 mM HEPES-buffered water (pH 7.0), (2) 30 mM ammonium formate, and (3) 1 M ammonium formate and 0.1 M formic acid. The radioactivity contained in each eluate and in the PI extract was counted by β -emission spectrometry, after the addition of 15 ml of Aquasol-2 scintillation cocktail (Packard Bioscience Ltd., Pangbourne, UK) to each vial. IP production was expressed as a percentage of the total radioactivity present in the sample (inositol plus GPI plus IP plus PI), because it was previously demonstrated that there is a good correlation between IP formation expressed in this way and that expressed per unit of tubule length (35,36).

Statistical Analyses

All data are presented as mean \pm SEM. Statistical comparisons were made using *t* tests for paired and unpaired samples and ANOVA, as appropriate. Statistical significance was taken as $P < 0.05$.

Chemicals

UDP, ADP, and ATP (disodium salts), as well as arterenol bitartrate (norepinephrine), carbamyl choline chloride (carbachol), angiotensin II, and 8-arginine vasopressin, were purchased from Sigma (Poole, Dorset, UK). Because commercially available UDP contains as much as 10% UTP, the UDP stock solution was treated for 1 h with hexokinase (10 U/ml), in the presence of 25 mM glucose.

Results

Distribution of P2Y₆ Receptor mRNA along the Rat Nephron

For each segment, P2Y₆ receptor mRNA expression was investigated in three or four extracts. Results obtained from one extract are illustrated in Figure 1. Strong signals were repeatedly observed in both the proximal tubule (PCT and proximal straight tubule) and the thick ascending limb (cortical thick ascending limb and MTAL), and less intense bands were observed in the DTL, CCD, and OMCD. No signal could be observed in the ATL or IMCD (Figure 1). The absence of detectable P2Y₆ signal in the ATL was not attributable to its thin diameter (and thus a smaller amount of mRNA in each PCR tube), because comparable GAPDH signals were obtained for the DTL, ATL, and OMCD (Figure 1B).

Effects of UDP on $[\text{Ca}^{2+}]_i$ in Isolated Nephron Segments

RT-PCR data indicated that P2Y₆ receptor mRNA is present in segments of the renal tubule, but they provide no information regarding expression of the protein. In the absence of an antibody against the P2Y₆ receptor, we measured UDP-stimulated changes in $[\text{Ca}^{2+}]_i$ in most segments containing mRNA, *i.e.*, the proximal tubule, the DTL, the MTAL, and the OMCD. As shown in Figure 2A, significant increases in $[\text{Ca}^{2+}]_i$ occurred in the proximal tubule. In contrast, the other segments were poorly responsive or unresponsive, although they were sensitive to other PLC-stimulating agonists used as controls (ATP or UTP for DTL and OMCD and angiotensin II for MTAL; results not shown). Compared with the results we obtained previously with ATP and ADP (23), the response to UDP in the proximal tubule was characterized by more intra- and interanimal variation (mean $[\text{Ca}^{2+}]_i$ increase, 365 ± 40 nM; $n = 33$). Nine of 42 tubules were observed to be insensitive to UDP, although they responded normally to either ATP (441 ± 74 nM, $n = 4$) or ADP (460 ± 81 nM, $n = 5$). The effect of UDP dose-dependently increased between 10 and 30 μM (Figure 2B). At all concentrations tested, the response was monophasic, with a single sharp peak before $[\text{Ca}^{2+}]_i$ returned to resting values (Figure 2C). In contrast, the responses to ATP and ADP were biphasic, consisting of a peak and then a lower plateau phase that was sustained throughout exposure to the agonist. Similarly, the responses to the other agonists used in this set of experiments (carbachol and norepinephrine) were biphasic (Figures 2C, 3, and 4).

Because the proximal tubule segments used in these initial experiments were microdissected at random from the kidney cortex and were not anatomically localized, it was possible that the scatter of UDP-induced $[\text{Ca}^{2+}]_i$ changes was physiologic and reflected different sensitivities of S1, S2, and S3 segments of the proximal tubule to this nucleotide. Therefore, subsequent experiments were performed with localized segments of proximal tubules. As stated in the Materials and Methods section, S3 segments were identified by anatomic criteria that could not be applied to S1 segments, because it is very difficult to microdissect proximal tubules attached to glomeruli in non-

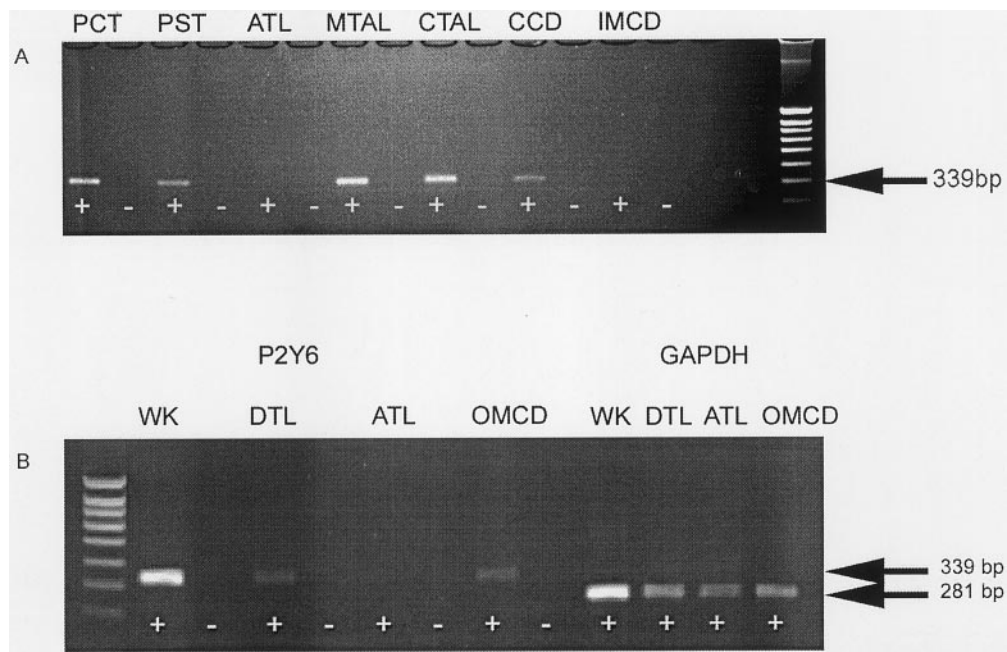


Figure 1. P2Y₆ receptor mRNA analysis. (A) Sample gel from one reverse transcription (RT)-PCR experiment, showing the distribution of P2Y₆ receptor mRNA in isolated segments of the rat nephron. PCT, proximal convoluted tubule; PST, proximal straight tubule; ATL, thin ascending limb; MTAL, medullary thick ascending limb; CTAL, cortical thick ascending limb; CCD, cortical collecting duct; IMCD, inner medullary collecting duct. + and –, samples assayed in the presence and absence of reverse transcriptase, respectively. (B) Comparison of P2Y₆ receptor and glyceraldehyde-3-phosphate dehydrogenase (GAPDH) mRNA expression in whole-kidney (WK), thin descending limb of Henle's loop (DTL), thin ascending limb of Henle's loop (ATL), and outer medullary collecting duct (OMCD) extracts. For whole-kidney samples, 1 μ g of total RNA (approximately 20 ng of mRNA) was used for RT-PCR; for DTL, ATL, and OMCD samples, we used 3 μ l of extract (*i.e.*, the mRNA extracted from 1-mm tubule length) in each tube. Note that the GAPDH signal was greater in whole-kidney samples than in tubule samples, whereas signals in ATL, DTL, and OMCD samples were comparable. This finding indicates that GAPDH signals did not reach saturation in the tubule samples and that comparable amounts of mRNA were used for RT-PCR for DTL, ATL, and OMCD samples.

collagenase-treated rat kidneys. As an alternative, we used a functional criterion based on results from previous studies, which demonstrated that changes in $[Ca^{2+}]_i$ in response to carbachol decrease from S1 to S3, whereas responses to norepinephrine remain constant (35). Therefore, responses to UDP, carbachol, and norepinephrine were always measured in the same segments, using carbachol as an index of localization and norepinephrine as an index of tubule viability. Figure 3 presents sample traces obtained for the S1, S2, and S3 segments. The mean UDP-induced responses were not statistically different between the S1 segment ($\Delta[Ca^{2+}]_i = 340 \pm 73$ nM, $n = 8$) and the S3 segment ($\Delta[Ca^{2+}]_i = 425 \pm 30$ nM, $n = 10$), a finding that suggests that the proximal tubule is responsive to UDP along its entire length.

Finally, we observed that two consecutive responses to UDP (30 μ M) did not occur in the same proximal tubule, even when stimulations were separated by 15 to 20 min of superfusion with control medium (data not shown). We took advantage of this result to examine whether this desensitization was specific for UDP or also applied to other nucleotides that had been previously demonstrated to stimulate PLC in this tubule segment (23). As illustrated by the trace in Figure 4, previous stimulation by UDP ($\Delta[Ca^{2+}]_i = 374 \pm 116$ nM, $n = 9$) prevented the effect of a second basolateral application of the nucleotide. However, these tubules remained sensitive to ADP

($\Delta[Ca^{2+}]_i = 440 \pm 118$ nM, $n = 6$), ATP ($\Delta[Ca^{2+}]_i = 333 \pm 89$ nM, $n = 3$), and norepinephrine ($\Delta[Ca^{2+}]_i = 404 \pm 63$ nM, $n = 5$), all of which were tested within the period of desensitization to UDP.

Effects of UDP on PI Metabolism in the PCT

To confirm that the effects of UDP on $[Ca^{2+}]_i$ were mediated via G-protein-coupled receptor activation of the PLC pathway, we assessed the effects of this agent on PI signaling in isolated segments of the proximal tubule. Production of IP was also investigated in the OMCD, a segment that expresses P2Y₆ receptor mRNA (Figure 1) but weakly responds to basolateral UDP superfusion (Figure 2). As previously reported for the PCT (35), approximately 80% of the total radioactivity was incorporated as PI. In contrast, only 5% of the total radioactivity appeared in the PI fraction in the OMCD, as reported for the thick ascending limb of Henle's loop (36).

For both segments, the percentages of radioactivity present in the IP pool under different experimental conditions are presented in Table 1. In the PCT, UDP (30 μ M) typically caused a fivefold increase in IP production, compared with basal values ($P < 0.01$). This increase was slightly, but not significantly, larger than that evoked by either ATP (used at the same concentration) or norepinephrine. In the OMCD, the P2Y₆ agonist also promoted a significant increase in the accu-

mulation of IP (three- to fourfold, $P < 0.05$), as did ATP (sixfold, $P < 0.01$) and arginine vasopressin (sevenfold, $P < 0.01$).

Discussion

In this study, we used the RT-PCR technique to demonstrate the expression of P2Y₆ receptor mRNA in whole kidney and we mapped the distribution of this receptor in specific renal tubular segments. P2Y₆ receptor mRNA was expressed mainly in the proximal tubule and thick ascending limb of Henle’s loop, but receptor transcripts were also identified in the DTL, the CCD, and the OMCD. Under our experimental conditions, there was no evidence for P2Y₆ receptor mRNA in either the ATL or the IMCD. The absence of a positive P2Y₆ receptor mRNA signal in the ATL is likely to be a real finding, because it was confirmed with different mRNA extracts, all of which demonstrated positive signals for GAPDH (see the example in Figure 1); moreover, the same extracts were previously dem-

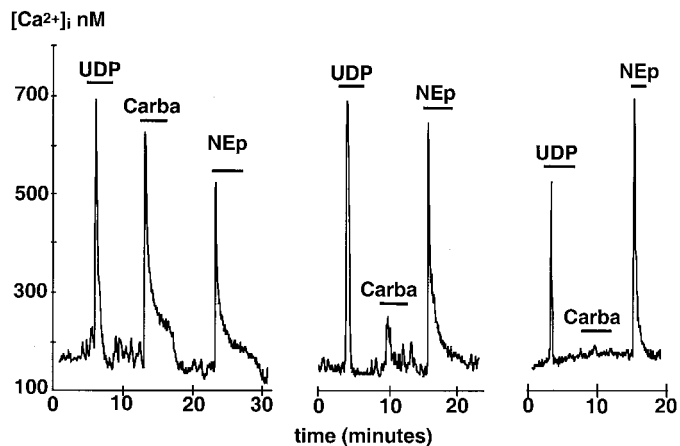


Figure 3. Representative traces, illustrating the effects of 30 μM UDP on [Ca²⁺]_i in different portions of the proximal tubule (S1, S2, and S3 segments). S3 segments were isolated from the cortex on the basis of anatomic criteria (see the Materials and Methods section); as explained in the Results section, S1 and S2 segments were identified on the basis of their different responsiveness to carbachol (Carba). Norepinephrine (NEp) was used as an index of tubule functional integrity.

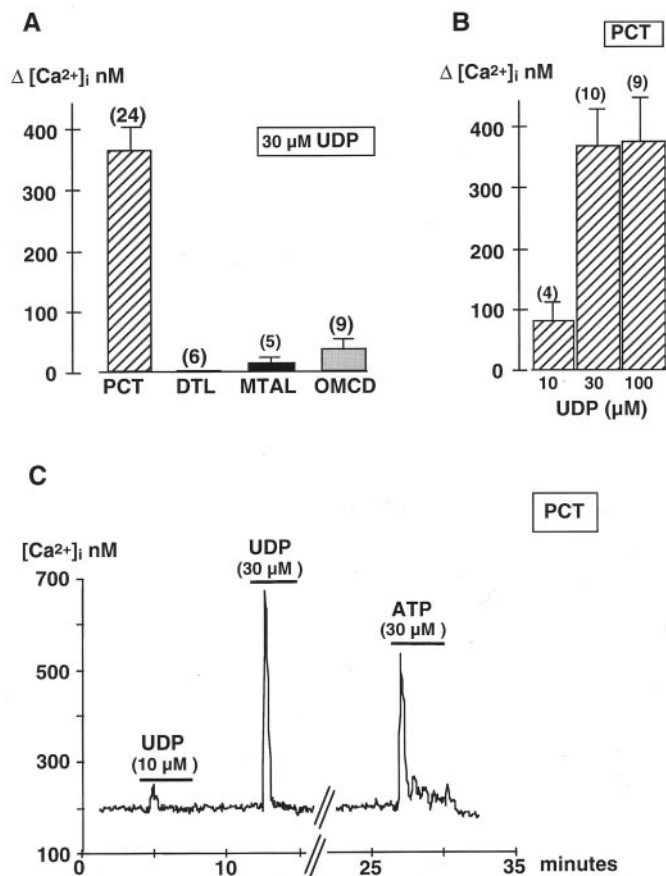


Figure 2. Pattern of UDP-induced intracellular calcium concentration ([Ca²⁺]_i) changes along the nephron. (A) [Ca²⁺]_i increases measured in nonlocalized PCT, DTL, MTAL, and OMCD. Bars correspond to mean ± SEM [Ca²⁺]_i increases (peak – basal levels) calculated for several tubules (numbers in parentheses) from at least four different rats. (B) Dose-dependent effects of UDP on [Ca²⁺]_i in PCT (mean ± SEM, *n* in parentheses). (C) Representative trace comparing the effects of UDP and ATP on [Ca²⁺]_i in PCT.

onstrated to be positive for P2Y₂ and P2Y₄ receptor mRNA (23).

The P2Y₆ receptor is functionally coupled to PLC, and receptor activation leads to transient increases in [Ca²⁺]_i in several cell types (5–7). We used this coupling to examine the functional expression of renal P2Y₆ receptors, by measuring changes in [Ca²⁺]_i during the application of UDP to the basolateral membrane. In all segments of the proximal tubule (S1,

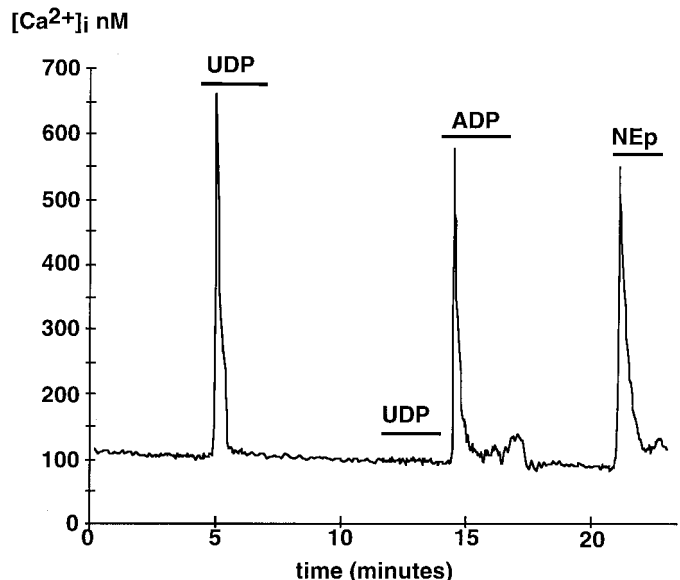


Figure 4. Representative trace, illustrating homologous desensitization of the calcium response to UDP after a single stimulation with the nucleotide (30 μM). Note that the responses to 30 μM ADP (an agonist specific for P2Y₁ receptors) and to 10 μM norepinephrine (NEp) were not blunted.

Table 1. Effects of phospholipase C-coupled agonists on IP accumulation in proximal tubules and OMCD^a

Condition	IP Production (% of Total Radioactivity)	
	Proximal Tubules	OMCD
Basal	1.76 ± 0.22	0.22 ± 0.04
UDP (30 μM)	9.82 ± 2.43 ^b	0.79 ± 0.40 ^c
ATP (30 μM)	7.06 ± 1.53 ^c	1.44 ± 0.40 ^b
Norepinephrine (10 μM)	6.78 ± 1.28 ^c	Not tested
AVP (100 nM)	Not tested	1.61 ± 0.36 ^b

^a Values are means ± SEM of 20 determinations (four rats) from samples incubated in the absence (basal level) or presence of UDP, ATP, or a positive control agent [norepinephrine and arginine vasopressin (AVP) for proximal tubules and outer medullary collecting ducts (OMCD), respectively] before determination of radioactivity in [³H]inositol-containing pools. For each experimental condition, inositol phosphate (IP) production was expressed as the percentage of total radioactivity incorporated in the sample.

^b $P < 0.01$ versus basal levels (one-way ANOVA).

^c $P < 0.05$.

S2, and S3), expression in the basolateral membrane was confirmed by the finding that peritubular UDP caused a dose-dependent increase in $[Ca^{2+}]_i$ (Figures 2 and 3). This probably represents (at least in part) release of calcium from intracellular stores, because IP production was also stimulated by UDP (Table 1). Unlike the proximal tubule, more distal tubular segments that expressed P2Y₆ receptor mRNA (Figure 1) did not respond to basolateral UDP superfusion with clear-cut increases in $[Ca^{2+}]_i$ (Figure 2); these findings were noted for the DTL, the whole thick ascending limb, the CCD, the IMCD, and the OMCD. These data may indicate that the receptor is only weakly coupled to PLC in these segments or that it is expressed exclusively in the luminal membrane. In support of the latter possibility, several studies have established the presence of luminal P2Y₆ receptors (12,13,15,22). However, our study did not allow us to address this question, because UDP had no access to the luminal membrane in our calcium experiments (see the Materials and Methods section). In contrast, the tubules used for the measurement of IP generation did have free open ends and were incubated for up to 15 min in the presence of UDP. Therefore, it is possible that the fourfold stimulation of IP production by UDP in the OMCD reflects activation of luminal receptors (Table 1), but contrary to this interpretation is the recent finding that UDP did not alter $[Ca^{2+}]_i$ when applied to the lumen of microperfused mouse CCD (28). However, there are species differences in the distribution of other P2Y receptors along the nephron, as well as their cellular localization. For example, levels of functional expression of P2Y₂ receptors in the basolateral membrane of the thick ascending limb are high in mice (25) but low in rats, despite the presence of mRNA (23), and evidence for luminal expression of P2Y₂ receptors has been observed in mouse CCD but not in rabbits (28). Such species differences could also

apply to the P2Y₆ receptor, and the development of specific antibodies to the P2Y₆ receptor would help address this issue.

Data in the literature have established that P2Y₁ receptors (23,26) and, to a lesser extent, P2Y₂ and/or P2Y₄ receptors (23) are expressed in the basolateral membrane of rat proximal tubules. This raises the question of whether UDP responses actually reveal the presence of an additional P2 receptor (Y or X) or whether they result from interactions with other P2 receptor subtypes. Four pieces of evidence support UDP-induced $[Ca^{2+}]_i$ changes as reliable indicators of the presence of the P2Y₆ receptor. The first is that UDP exposure was associated with increased IP production, a finding that cannot be accounted for by UDP interactions with ionotropic P2X receptors. The second is that tubular segments that were previously demonstrated to express PLC-coupled P2Y₂/P2Y₄ receptors (DTL and OMCD) and P2Y₁ receptors (OMCD) in their basolateral membranes (23) were insensitive to UDP (Figure 1). The third is that the transient monophasic increases in $[Ca^{2+}]_i$ elicited by UDP in proximal tubules are unlike the biphasic responses to other P2Y receptor agonists, such as ATP and ADP (Figures 2 to 4). This suggests that renal P2Y₆ receptors may be coupled to different effector pathways, compared with P2Y₁ and P2Y₂ receptors. Indeed, a recent study reported that P2Y₆ receptors expressed in *Xenopus* oocytes are coupled to only one class of G-protein, whereas P2Y₂ receptors are coupled to two (37). There is also a large body of evidence indicating that different P2Y receptor subtypes expressed in the same cells activate different signal transduction pathways [see the report by Communi *et al.* (9)]. The fourth piece of evidence is our previous demonstration that no desensitization occurred when several successive stimulations with maximal concentrations of ATP and/or ADP were administered to proximal tubules (23). In contrast, in our present experiments we observed that a single UDP stimulation prevented further responses to this nucleotide but did not affect the ability of the proximal tubule to respond to ATP or ADP (Figure 4). Taken together, the data suggest that the response to UDP involves a receptor that is distinct from the ADP- and ATP-sensitive P2Y₁ subtype.

We have not analyzed the mechanisms underlying the desensitization of the calcium response to UDP, *i.e.*, whether it occurs at the receptor level or further along the PLC/ $[Ca^{2+}]_i$ pathway. Whatever the mechanism, this desensitization process, which seems to be specific for the P2Y₆ receptor, may explain why the effects of UDP on $[Ca^{2+}]_i$ were more variable in magnitude than were those of ATP and ADP (see the Results section). Little is presently known regarding the source and identity of the natural ligands for the P2Y₆ receptor (1,9). It could be that abnormal nucleotide release, because of the conditions of the study animals and/or the tubule preparations, accounts for the variability in UDP-induced calcium effects; such variation in UDP effects has already been described for pancreatic duct cells (22). Preferential desensitization of P2Y₆ receptor-induced responses, compared with P2Y₂ receptor-induced calcium responses, has also been reported for nasal epithelium (13).

The maximal ATP-induced effects on IP production and

[Ca²⁺]_i were in the range of those induced by UDP or ADP alone, which may mean that the P2Y₆ receptor is only weakly sensitive to ATP in rat proximal tubules, as it is when expressed in *Xenopus* oocytes (5) and other cell types (6,15,20,38). If this is true, then the effects of ATP must reflect mainly interactions with the basolateral P2Y₁ receptor. Another possibility is that the P2Y₆ and P2Y₁ receptor subtypes are present in the same cells and hydrolyze the same pool of membrane PI and that a single stimulation of either one at high concentrations is sufficient to induce maximal effects on IP production and intracellular calcium release. These alternatives are not mutually exclusive, because we already have evidence for such a coupling between P2Y₁ and P2Y₂ receptors in the same cell type in the rat OMCD (23). If P2Y₆, P2Y₁, P2Y₂, and/or P2Y₄ receptors are coexpressed in the basolateral membrane of the same proximal tubule cells, then the important question is whether these nucleotides can induce similar or distinct physiologic responses (9). Perhaps there is some necessary functional overlap or redundancy. Published data from studies on the secretory epithelium of upper respiratory airways and exocrine glands indicate that different P2Y receptors coexpressed in the same cells all stimulated PLC and activated chloride currents (9). Results obtained in P2Y₂ receptor-deficient mice indicate that the apical P2Y₆ receptor can substitute for the inactivated P2Y₂ receptor to regulate chloride secretion in the gallbladder (20). However, in addition to this common regulatory pathway, other data indicate that different (10,37) or the same (38) P2Y receptors can couple to different G-proteins in the same cell to activate different isoforms of PLC (39) and thus regulate different effectors (37,38). This may result in synergistic or opposing effects on cell functions. G-protein-dependent inhibition of calcium and potassium currents by P2Y₆ receptors is thought to exert synergistic effects on neuronal excitability in rat sympathetic neurons. Conversely, ATP and ADP are known to induce opposite effects on platelet aggregation. From these observations, it is clear that the interactions among different P2Y receptors are specific for each cell type, depending on the nature of cellular components and on whether the receptor is targeted to the luminal or basolateral membrane.

Acknowledgments

The Wellcome Trust and the Medical Research Council supported this work. We thank the St. Peter's Research Trust for Kidney, Bladder, and Prostate Research for additional support.

References

- Lazarowski ER, Harden TK: Quantitation of extracellular UTP using a sensitive enzymatic assay. *Br J Pharmacol* 127: 1272–1278, 1999
- Chen ZP, Krull N, Xu S, Levy A, Lightman S: Molecular cloning and functional characterization of a rat pituitary G protein-coupled adenosine triphosphate (ATP) receptor. *Endocrinology* 137: 1833–1839, 1996
- Bogdanov YD, Wildman SS, Clements MP, King BF, Burnstock G: Molecular cloning and characterization of rat P2Y₄ nucleotide receptor. *Br J Pharmacol* 124: 428–430, 1998
- Webb TE, Henderson DJ, Roberts JA, Barnard EA: Molecular cloning and characterization of the rat P2Y₄ receptor. *J Neurochem* 71: 1348–1357, 1998
- Chang K, Hanaoka K, Kumada M, Takuwa Y: Molecular cloning and functional analysis of a novel P₂ nucleotide receptor. *J Biol Chem* 270: 26152–26158, 1995
- Communi D, Parmentier M, Boeynaems JM: Cloning, functional expression and tissue distribution of the human P2Y₆ receptor. *Biochem Biophys Res Commun* 222: 303–308, 1996
- Nicholas RA, Watt WC, Lazarowski ER, Li Q, Harden K: Uridine nucleotide selectivity of three phospholipase C-activating P2 receptors: Identification of a UDP-selective, a UTP-selective, and an ATP- and UTP-specific receptor. *Mol Pharmacol* 50: 224–229, 1996
- Ralevic V, Burnstock G: Receptors for purines and pyrimidines. *Pharmacol Rev* 50: 413–492, 1998
- Communi D, Janssens R, Suarez-Huerta N, Robaye B, Boeynaems JM: Advances in signalling by extracellular nucleotides: The role and transduction mechanisms of P2Y receptors. *Cell Signal* 12: 351–360, 2000
- Firestein BL, Xing M, Hughes RJ, Corvera CU, Insel PA: Heterogeneity of P2U and P2Y-purinergic receptor regulation of phospholipases in MDCK cells. *Am J Physiol* 271: F610–F618, 1996
- Gordjani N, Nitschke R, Greger R, Leipziger J: Capacitive calcium entry (CCE) induced by luminal and basolateral ATP in polarized MDCK-C7 cells is restricted to the basolateral membrane. *Cell Calcium* 22: 121–128, 1997
- Ko WH, Wilson SM, Wong PYD: Purine and pyrimidine nucleotide receptors in the apical membrane of equine cultured epithelia. *Br J Pharmacol* 121: 150–156, 1997
- Lazarowski ER, Paradiso AM, Watt WC, Harden TK, Boucher RC: UDP activates a mucosal-restricted receptor on human nasal epithelial cells that is distinct from the P2Y₂ receptor. *Proc Natl Acad Sci USA* 94: 2599–2603, 1997
- Banderali U, Brochiero E, Lindenthal S, Raschi C, Bogliolo S, Ehrenfeld J: Control of apical membrane chloride permeability in the renal A6 cell line by nucleotides. *J Physiol (Lond)* 519: 737–751, 1999
- Ko WH, Law VW, Wong HY, Wilson SM: The simultaneous measurement of epithelial ion transport and intracellular free Ca²⁺ in cultured equine sweat gland secretory epithelium. *J Membr Biol* 170: 205–211, 1999
- McCoy DE, Taylor AL, Kudlow BA, Karlson K, Slattery MJ, Schwiebert LM, Schwiebert EM, Stanton BA: Nucleotides regulate NaCl transport in mIMCD-K2 cells via P2X and P2Y purinergic receptors. *Am J Physiol* 277: F552–F559, 1999
- Cuffe JE, Bielfeld-Ackermann A, Thomas J, Leipziger J, Korbmayer C: ATP stimulates Cl⁻ secretion and reduces amiloride-sensitive Na⁺ absorption in M-1 mouse cortical collecting duct cells. *J Physiol (Lond)* 524: 77–90, 2000
- Lee MG, Zeng W, Muallem S: Characterization and localization of P2 receptors in rat submandibular gland acini and duct cells. *J Biol Chem* 272: 32951–32955, 1997
- Kerstan D, Gordjani N, Nitschke R, Greger R, Leipziger J: Luminal ATP induces K⁺ secretion via a P2Y₂ receptor in rat distal colonic mucosa. *Pfluegers Arch* 436: 712–716, 1998
- Cressman VL, Lazarowski E, Homolya L, Boucher RC, Koller BH, Grubb BR: Effect of loss of P2Y₂ receptor gene expression on nucleotide regulation of murine epithelial Cl⁻ transport. *J Biol Chem* 274: 26461–26468, 1999

21. Hede SE, Amstrup J, Christoffersen BC, Novak I: Purinoceptors evoke different electrophysiological responses in pancreatic ducts. *J Biol Chem* 274: 31784–31791, 1999
22. Luo X, Zheng W, Yan M, Lee MG, Muallem S: Multiple functional P2X and P2Y receptors in the luminal and basolateral membranes of pancreatic duct cells. *Am J Physiol* 277: C205–C215, 1999
23. Bailey MA, Imbert-Teboul M, Turner C, Burnstock G, Unwin RJ: Axial distribution and characterisation of basolateral P2Y receptors along the rat renal tubule. *Kidney Int* 58: 1893–1901, 2000
24. Ecelbarger CA, Maeda Y, Gibson C, Knepper MA: Extracellular ATP increases intracellular calcium in rat terminal collecting duct via a nucleotide receptor. *Am J Physiol* 267: F998–F1006, 1994
25. Paulais M, Baudoin-Legros M, Teulon J: Extracellular ATP and UTP trigger calcium entry in mouse cortical thick ascending limbs. *Am J Physiol* 268: F496–F502, 1995
26. Cha SH, Sekine T, Endou H: P2 purinoceptor localization along the rat nephron and evidence suggesting existence of subtypes P2Y₁ and P2Y₂. *Am J Physiol* 274: F1006–F1014, 1998
27. Kishore BK, Ginns SM, Krane CM, Nielsen S, Knepper MA: Cellular localization of P2Y₂ purinoceptor in rat inner medulla and lung. *Am J Physiol* 278: F43–F51, 2000
28. Deetjen P, Thomas J, Lehrmann H, Kim SJ, Leipziger J: The luminal P2Y receptor in the isolated perfused mouse cortical collecting duct. *J Am Soc Nephrol* 11: 1798–1806, 2000
29. Wilson SM, Law VW, Pediani JD, Allen EA, Wilson G, Khan ZE, Ko WH: Nucleotide-evoked calcium signals and anion secretion in equine cultured epithelia that express apical P2Y₂ receptors and pyrimidine nucleotide receptors. *Br J Pharmacol* 124: 832–838, 1998
30. Elalouf JM, Buhler JM, Tessiot C, Bellanger AC, Dublineau I, De Rouffignac C: Predominant expression of beta 1-adrenergic receptor in the thick ascending limb of rat kidney: Absolute mRNA quantitation by reverse transcription and polymerase chain reaction. *J Clin Invest* 91: 264–272, 1993
31. Chomczynski P, Sacchi N: Single-step method of RNA isolation by acid guanidinium thiocyanate-phenol-chloroform extraction. *Anal Biochem* 162: 156–159, 1987
32. Champigneulle A, Siga E, Vassent G, Imbert-Teboul M: A V2-like vasopressin receptor mobilizes intracellular Ca²⁺ in rat medullary collecting tubules. *Am J Physiol* 265: F35–F45, 1993
33. Gryniewicz G, Poenie M, Tsien RY: A new generation of Ca²⁺ indicators with greatly improved fluorescence properties. *J Biol Chem* 260: 3440–3450, 1985
34. Meneton P, Bloch-Faure M, Guillon G, Chabardes D, Morel F, Rajerison RM: Cholinergic stimulation of phosphoinositide metabolism in isolated rat glomeruli. *Am J Physiol* 262: F256–F266, 1992
35. Meneton P, Imbert-Teboul M, Bloch-Faure M, Rajerison RM: Cholinergic agonists increase phosphoinositide metabolism and cell calcium in isolated rat renal proximal tubule. *Am J Physiol* 271: F382–F390, 1996
36. De Jesus Ferreira MC, Helies-Toussaint C, Imbert-Teboul M, Bailly C, Verbavatz JM, Bellanger AC, Chabardes D: Co-expression of a Ca²⁺-inhibitable adenylyl cyclase and of a Ca²⁺-sensing receptor in the cortical thick ascending limb cell of the rat kidney: Inhibition of hormone-dependent cAMP accumulation by extracellular Ca²⁺. *J Biol Chem* 273: 15192–15202, 1998
37. Mosbacher J, Maier R, Fakler B, Glatz A, Crespo J, Bilbe G: P2Y receptor subtypes differentially couple to inwardly-rectifying potassium channels. *FEBS Lett* 436: 104–110, 1998
38. Filippov AK, Webb TE, Barnard EA, Brown DA: Dual coupling of heterologously-expressed rat P2Y₆ nucleotide receptors to N-type Ca²⁺ and M-type K⁺ currents in rat sympathetic neurones. *Br J Pharmacol* 126: 1009–1017, 1999
39. Murthy KS, Makhoul GM: Coexpression of ligand-gated P2X and G protein-coupled P2Y receptors in smooth muscle: Preferential activation of P2Y receptors coupled to phospholipase C (PLC)-β1 via Gαq/11 and to PLC-β3 via Gβγ3. *J Biol Chem* 273: 4695–4704, 1998